TUM-HEP-552/04

Precision spectroscopy with reactor anti-neutrinos

Patrick Huber[a] **and Thomas Schwetz**[b]

Physik–Department, Technische Universität München
James–Franck–Strasse, D–85748 Garching, Germany

Abstract

In this work we present an accurate parameterization of the anti-neutrino flux produced by the isotopes ^{235}U, ^{239}Pu, and ^{241}Pu in nuclear reactors. We determine the coefficients of this parameterization, as well as their covariance matrix, by performing a fit to spectra inferred from experimentally measured beta spectra. Subsequently we show that flux shape uncertainties play only a minor role in the KamLAND experiment, however, we find that future reactor neutrino experiments to measure the mixing angle θ_{13} are sensitive to the fine details of the reactor neutrino spectra. Finally, we investigate the possibility to determine the isotopic composition in nuclear reactors through an anti-neutrino measurement. We find that with a 3 month exposure of a one ton detector the isotope fractions and the thermal reactor power can be determined at a few percent accuracy, which may open the possibility of an application for safeguard or non-proliferation objectives.

[a]Email: phuber@ph.tum.de
[b]Email: schwetz@ph.tum.de

1 Introduction

Experiments at nuclear reactors have a long tradition in neutrino physics. Starting from the experimental discovery of the neutrino at the legendary Cowan-Reines experiment [1], many measurements at nuclear power plants have provided valuable information about neutrinos. For example, the results of the Gösgen [2], Bugey [3], Palo Verde [4], and CHOOZ [5] experiments have lead to stringent limits on electron anti-neutrino disappearance. Reactor neutrino experiments have become very prominent again due to the outstanding results of the KamLAND experiment [6,7]. For a review on reactor neutrino experiments, see Ref. [8]. Recently the possibility to determine the last unknown lepton mixing angle θ_{13} by a reactor neutrino experiment with a near and far detector is actively investigated (see Ref. [9] and references therein). Building on the experience gathered in oscillation experiments ideas of "applied neutrino physics" appeared [10–12]: A detector close to a nuclear reactor could be used for reactor monitoring, either for improving the reliability of operation of power reactors or as a method to accomplish certain safeguard requirements in the context of international treaties for arms control and non-proliferation of weapons of mass destruction.

The standard detection process for reactor neutrinos is inverse beta decay:

$$\bar{\nu}_e + p \to e^+ + n\,. \tag{1}$$

The cross section $\sigma(E_\nu)$ for this process is very well known [13], at an accuracy better than 1%. Per fission roughly 6 electron anti-neutrinos are produced (see *e.g.* Ref. [8]), with energies peaked around 1 MeV. However, for inverse beta decay only neutrinos with energies above the threshold of 1.8 MeV are relevant. In nuclear reactors electron anti-neutrinos in that energy range are produced dominantly by the beta decay of the fission products from the four isotopes $\ell = {}^{235}\mathrm{U}$, ${}^{239}\mathrm{Pu}$, ${}^{238}\mathrm{U}$, ${}^{241}\mathrm{Pu}$.[1] We denote the flux from the isotope ℓ by $\phi_\ell(E_\nu)$ in units of anti-neutrinos per fission and MeV. In Table 1 the total number of $\bar{\nu}_e$ per fission above 1.8 MeV is given for ${}^{235}\mathrm{U}$, ${}^{239}\mathrm{Pu}$, ${}^{241}\mathrm{Pu}$, and ${}^{238}\mathrm{U}$.

Accurate information on the anti-neutrino flux from ${}^{235}\mathrm{U}$, ${}^{239}\mathrm{Pu}$, and ${}^{241}\mathrm{Pu}$ can be obtained by the measurement of the beta spectra from the exposure of these isotopes to thermal neutrons [16–18]. Subsequently these beta spectra have to be converted into anti-neutrino spectra, taking into account the large number of beta branches involved. These spectra are in excellent agreement with the direct observation of the anti-neutrino spectrum at the Bugey [19] and Rovno [14] reactors. The errors on these fluxes are at the level of a few percent. Since modern reactor neutrino experiments aim at precisions at this level, a proper treatment of the flux uncertainties becomes necessary. For ${}^{238}\mathrm{U}$, which does only undergo fast neutron fission, no similar measurements exist, and one has to rely on theoretical calculations [20,21].

In absence of neutrino oscillations the number of positron events for a measurement time

[1] The next to leading contributions come from the isotopes ${}^{240}\mathrm{Pu}$ and ${}^{242}\mathrm{Pu}$ and are of the order 0.1% or less [8]. Further sub-leading effects are the beta decay of ${}^{239}\mathrm{U}$, ${}^{239}\mathrm{Np}$, ${}^{237}\mathrm{U}$ (produced by radiative neutron capture), and corrections to the spectra from fission fragments due to neutron absorption by these fragments [14]. These effects are relevant for the low energy part of the anti-neutrino spectrum $E_\nu \lesssim 2$ MeV and will be neglected in the following. See also Ref. [15].

ℓ	N_ℓ^ν	E_ℓ [MeV]
^{235}U	$1.92(1 \pm 0.019)$	201.7 ± 0.6
^{238}U	$2.38(1 \pm 0.020)$	205.0 ± 0.9
^{239}Pu	$1.45(1 \pm 0.021)$	210.0 ± 0.9
^{241}Pu	$1.83(1 \pm 0.019)$	212.4 ± 1.0

Table 1: Total number of $\bar{\nu}_e$ per fission above 1.8 MeV (see Section 3 for details) and energy release per fission (reproduced from Table 2 of Ref. [5]) for the isotopes relevant in nuclear reactors.

T in a given positron energy bin i can be calculated by

$$N_i = \frac{n_p T}{4\pi L^2} \sum_\ell N_\ell^{\rm fis} \int {\rm d}E_\nu \, \sigma(E_\nu) \, \phi_\ell(E_\nu) \, R_i(E_\nu) \, . \tag{2}$$

Here n_p is the number of protons in the detector, L is the distance between reactor core and detector, and $R_i(E_\nu)$ is the detector response function for the bin i (including energy resolution and efficiencies). If the initial composition of the reactor fuel is known, the number of fissions per second $N_\ell^{\rm fis}$ of each isotope ℓ can be calculated accurately (better than 1% [8]) at each burn-up stage by core simulation codes. The thermal power output P of the reactor is given by $P = \sum_\ell N_\ell^{\rm fis} E_\ell$, where E_ℓ is the energy release per fission for the isotope ℓ, see Table 1. Since the errors on E_ℓ are less than 0.5% we will neglect in the following the uncertainty induced by them. Defining the relative contribution of the element ℓ to the total power[2] f_ℓ, the $N_\ell^{\rm fis}$ can be expressed by P and Eq. (2) becomes

$$N_i = \frac{n_p T}{4\pi L^2} \, P \sum_\ell \frac{f_\ell}{E_\ell} \int {\rm d}E_\nu \, \sigma(E_\nu) \, \phi_\ell(E_\nu) \, R_i(E_\nu) \quad \text{with} \quad f_\ell \equiv \frac{N_\ell^{\rm fis} E_\ell}{P} \, . \tag{3}$$

The aim of the present work is to consider various aspects of reactor neutrino spectroscopy, with a main emphasis on issues related to the emitted anti-neutrino flux. First, in Section 2 we present a phenomenological parameterization for the anti-neutrino fluxes ϕ_ℓ based on a polynomial of order 5. We show that in many situations existing parameterizations [22] are not accurate enough to describe the reactor neutrino spectrum at the required level of precision. In addition, in Section 3 we give a detailed consideration of the errors associated to the reactor anti-neutrino spectrum and provide them in a suitable form for implementation in data analyses. In the following we consider the implications of uncertainties of various quantities appearing in Eq. (3) for several experimental configurations. In Section 4 we discuss the impact of errors on P, f_ℓ, and ϕ_ℓ for the KamLAND experiment, whereas in Section 5 we discuss the relevance of our new parameterization of ϕ_ℓ and its errors for future reactor experiments to measure θ_{13}. In Section 6 we consider the potential of an anti-neutrino detector close to a reactor: In Section 6.1 we discuss the improvement on the flux uncertainties from a near detector, and in Section 6.2 we investigate the possibility of reactor monitoring by using the anti-neutrino measurement. In contrast to previous studies [10–12] we employ full spectral information, which allows the determination of the isotopic content of a reactor, *i.e.* the fractions f_ℓ, as well as the reactor power P without any external information. We conclude in Section 7.

[2]The *power* fractions f_ℓ must not be confused with the relative *fission* contributions $f_\ell^{\rm fis} \equiv N_\ell^{\rm fis} / \sum_\ell N_\ell^{\rm fis}$. In this case one would obtain $N_\ell^{\rm fis} = f_\ell^{\rm fis} P / \langle E \rangle$, where the mean energy per fission is given by $\langle E \rangle = \sum_\ell f_\ell^{\rm fis} E_\ell$.

2 A parameterization for the reactor anti-neutrino flux

In Refs. [16,17] anti-neutrino spectra from the fission products of ^{235}U, ^{239}Pu, and ^{241}Pu are determined by converting the precisely measured associated beta spectra. In this section we propose a phenomenological parameterization for the reactor anti-neutrino flux, based on these measurements. Similar as in Ref. [22] we parameterize the spectrum of a given element using a polynomial:

$$\phi_\ell(E_\nu) = \exp\left(\sum_{k=1}^{K_\ell} a_{k\ell} E_\nu^{k-1}\right) . \tag{4}$$

The coefficients $a_{k\ell}$ are determined by a fit to the data of Refs. [16, 17]. To this aim we minimize the following χ^2-function:

$$\chi^2 = \sum_{i,j} D_i S_{ij}^{-1} D_j \quad \text{with} \quad D_i \equiv \sum_{k=1}^{K_\ell} a_{k\ell} (E_\nu^{(i)})^{k-1} - \ln \phi_\ell^{(i)} , \tag{5}$$

where $E_\nu^{(i)}$ and $\phi_\ell^{(i)} \equiv \phi_\ell(E_\nu^{(i)})$ are the values of the neutrino energy and the corresponding anti-neutrino flux, respectively, provided in the tables of Refs. [16, 17] for values of the neutrino energy E_ν ranging from 1.5 to 9.5 MeV in steps of 0.25 MeV. Since we are fitting the logarithm of the flux the covariance matrix S_{ij} contains relative errors of the $\phi_\ell^{(i)}$. For the diagonal elements S_{ii} we take the errors as given in the tables of Refs. [16,17] (converted from 90% CL to 1σ and squared), which contain the statistical error from the beta spectrum measurement, a systematic error on the overall calibration, and a systematic error from the conversion from beta to anti-neutrino spectrum. The off-diagonal elements are obtained from the error on the absolute calibration, which is taken as fully correlated: $S_{ij} = \sigma_i^{\rm cal}\sigma_j^{\rm cal}$ for $i \neq j$. The errors $\sigma_i^{\rm cal}$ are given at two calibration energies for each isotope in Refs. [16–18], and we interpolate linearly between these reference points. Note that this procedure assumes that the systematical errors from the conversion from beta to anti-neutrino spectrum are completely uncorrelated between different energies.

First we have performed a fit of a polynomial of second order ($K_\ell = 3$). The resulting coefficients $a_{k\ell}$ are given in Table 2 in Appendix A, and are in reasonable agreement with the ones obtained in Ref. [22] (some deviations appear for ^{241}Pu). However, we find that the quality of this three parameter fit is very bad for all three isotopes (the χ^2 is given in Figure 1 in the following). We conclude that at the level of precision provided by the errors the data cannot be described with sufficient accuracy by the polynomial of order 2. We have checked that a reasonable fit is obtained for all three elements only by going up to a polynomial of order 5, corresponding to $K_\ell = 6$ parameters. The best fit coefficients $a_{k\ell}$ are given in Table 3 in Appendix A, and the corresponding anti-neutrino spectra are available in computer readable format at the web-page Ref. [23].

Our fit is illustrated in Figure 1, where we show the resulting spectra for the 3 and 6 parameter fits in comparison to the data. Large differences between the 3 and 6 parameter fit are visible by eye only for the high energy region, where the spectra are very small and errors are large. However, comparing the corresponding χ^2-values $\chi^2_{(3)}$ and $\chi^2_{(6)}$ given in the figure it is obvious that the 6 parameters are necessary to obtain a reasonable goodness-of-fit. In the lower panels we show the residuals of the fit, *i.e.*, for each data point i we plot $(\phi^{(i)}_{\ell\,\rm data} - \phi^{(i)}_{\ell\,\rm fit})/\sigma_i$, where the error is obtained from the covariance matrix S by $\sigma_i =$

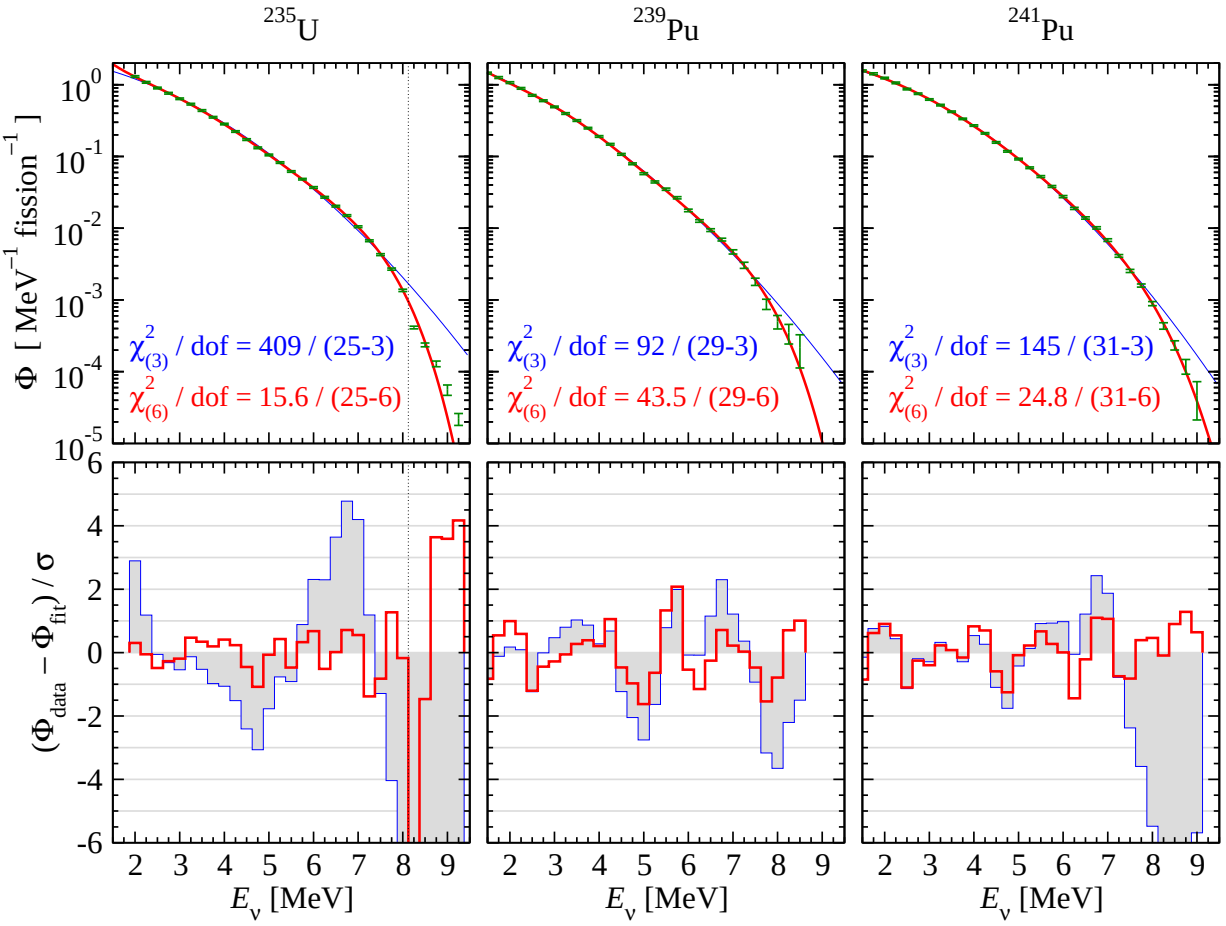

Figure 1: (Color online) Illustration of the fit to the data on the anti-neutrino spectra from ^{235}U [16], ^{239}Pu [17], and ^{241}Pu [17]. The thick/red curves correspond to a 6 parameter fit (polynomial of order 5), whereas the thin/blue curves correspond to a 3 parameter fit (polynomial of order 2). Also shown are the data with their 1σ error bars and the χ^2 per degree of freedom (number of data points minus fitted parameters). In the lower panels we show the residuals of the fits. Note that because of correlations the shown residuals do not add up to the given χ^2-values. The data points to the right of the dotted line in the ^{235}U-panels are excluded from the fit.

$\phi^{(i)}_{\ell\,\mathrm{data}}\sqrt{S_{ii}}$. Note that because of correlations between the $\phi^{(i)}_{\ell\,\mathrm{data}}$ these residuals do not add up to the total χ^2. For ^{235}U the 3 parameter fit shows rather large residuals over the full energy range. Since this isotope gives the main contribution to the reactor anti-neutrino flux it is very important to model its neutrino spectrum correctly. Let us note that we exclude six data points at high neutrino energies from the fit. The change in the spectral shape around 8 MeV [16] cannot be fitted very well by the polynomial,[3] although by accident the 6 parameter fit gives a reasonable approximation also in this energy range. Also for ^{241}Pu the high energy range $E_\nu \gtrsim 7$ MeV is important. In this case it is possible to obtain a good fit from the polynomial of order 5 even including the high energy part.

[3] In Ref. [14] a term of order E_ν^{10} is introduced to model this sharp falloff.

3 Quantifying the anti-neutrino flux uncertainties

In this section we discuss in detail the uncertainties on the reactor anti-neutrino fluxes. In Table 3 in Appendix A we show the errors $\delta a_{k\ell}$ on the coefficients of the polynomial as well as their correlation matrix $\rho^{\ell}_{kk'}$, as obtained from the fit to the measured beta spectra. Hence, the covariance matrix V^{ℓ} for the coefficients can be obtained by

$$V^{\ell}_{kk'} = \delta a_{k\ell}\, \delta a_{k'\ell}\, \rho^{\ell}_{kk'} \,. \tag{6}$$

From the table one observes that for a given element the coefficients are strongly correlated or anti-correlated, since for most elements of the correlation matrix we obtain $|\rho^{\ell}_{kk'}| \approx 1$. Therefore, we perform a rotation in the space of the $a_{k\ell}$, such that the covariance matrix becomes diagonal. Let us for each isotope introduce new coefficients $c_{k\ell}$ by

$$a_{k\ell} = \sum_{k'} \mathcal{O}^{\ell}_{k'k}\, c_{k'\ell} \,, \tag{7}$$

where the orthogonal matrix $\mathcal{O}^{\ell}$ is defined by

$$\mathcal{O}^{\ell}\, V^{\ell}\, (\mathcal{O}^{\ell})^T = \mathrm{diag}\left[(\delta c_{k\ell})^2\right] \,. \tag{8}$$

Hence, the $\delta c_{k\ell}$ are the (uncorrelated) errors on the coefficients $c_{k\ell}$. Using Eqs. (4) and (7) the anti-neutrino flux for the isotope ℓ can be written as

$$\phi_{\ell}(E_\nu) = \exp\left[\sum_{k=1}^{K_\ell} c_{k\ell}\, p^{\ell}_k(E_\nu)\right] \,, \tag{9}$$

where $p^{\ell}_k(E_\nu)$ is a polynomial of E_ν given by

$$p^{\ell}_k(E_\nu) = \sum_{k'=1}^{K_\ell} \mathcal{O}^{\ell}_{kk'} E_\nu^{k'-1} \,. \tag{10}$$

These polynomials describe the uncorrelated contributions to the error on the anti-neutrino flux. For example, let us consider some observable X, involving the anti-neutrino flux in the following way: $X = \int \mathrm{d}E_\nu\, h(E_\nu)\, \phi_{\ell}(E_\nu)$, where $h(E_\nu)$ is some function of the neutrino energy. Then the error contribution from the coefficient $c_{k\ell}$ is given by

$$\delta X = \delta c_{k\ell}\, \frac{\partial X}{\partial c_{k\ell}} = \int \mathrm{d}E_\nu\, h(E_\nu)\, \phi_{\ell}(E_\nu)\, \delta c_{k\ell}\, p^{\ell}_k(E_\nu) \,. \tag{11}$$

Hence, the product $\delta c_{k\ell}\, p^{\ell}_k(E_\nu)$ is a measure for the importance of the error $\delta c_{k\ell}$ for any observable. In the upper panel of Figure 2 we show the polynomials Eq. (10) weighted by the corresponding error for ^{235}U. For ^{239}Pu and ^{241}Pu we obtain very similar results. One observes that in the relevant range of the anti-neutrino energy the flux uncertainties are at the level of 2%. The weighted polynomials $\delta c_{k\ell}\, p^{\ell}_k(E_\nu)$ for the isotopes ^{235}U, ^{239}Pu, ^{241}Pu are available in computer readable format at the web-page Ref. [23]. Once these functions are known, the flux uncertainties on any observable can be included similar to Eq. (11).

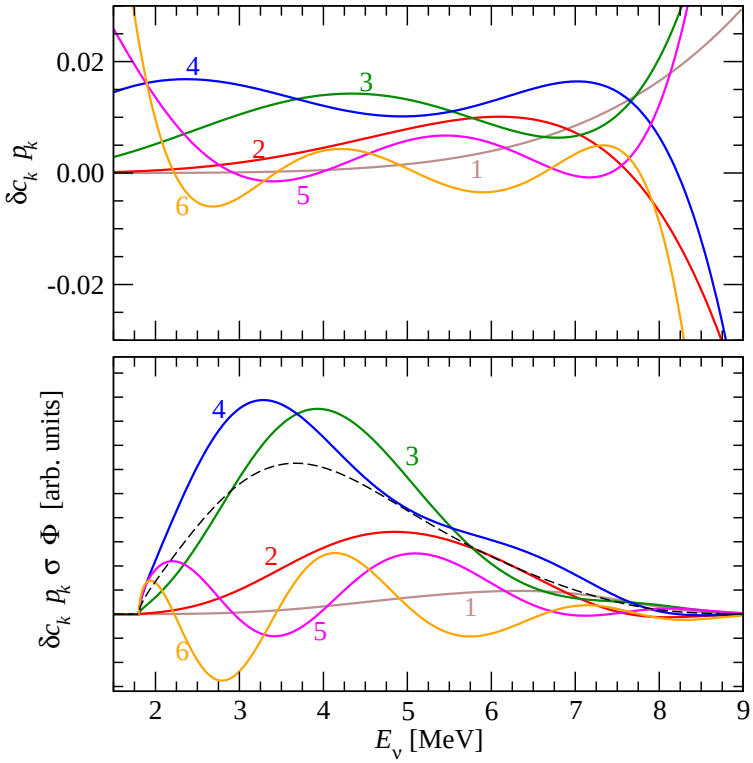

Figure 2: (Color online) Uncorrelated anti-neutrino flux uncertainties for ^{235}U. The upper panel shows the polynomials $p_k^\ell(E_\nu)$ given in Eq. (10) multiplied by the corresponding error $\delta c_{k\ell}$. The lower panel shows the functions $\delta c_{k\ell}\, p_k^\ell(E_\nu)\, \sigma(E_\nu)\, \phi_\ell(E_\nu)$, where $\sigma(E_\nu)$ is the detection cross section. The dashed curve corresponds to $\sigma(E_\nu)\, \phi_\ell(E_\nu)/100$.

As first simple application let us mention how one can calculate the number of anti-neutrinos per fission N_ℓ^ν above the threshold and its uncertainty, as given in Table 1. Given the best fit parameters and their covariance matrix for ^{235}U, ^{239}Pu, ^{241}Pu we readily obtain

$$N_\ell^\nu = \int_{1.8\,\mathrm{MeV}}^{\infty} \phi_\ell(E_\nu)\, \mathrm{d}E_\nu\,, \qquad (\delta N_\ell^\nu)^2 = \sum_{kk'} \frac{\partial N_\ell^\nu}{\partial a_{k\ell}} \frac{\partial N_\ell^\nu}{\partial a_{k'\ell}} V_{kk'}^\ell = \sum_k \left(\frac{\partial N_\ell^\nu}{\partial c_{k\ell}}\, \delta c_{k\ell} \right)^2 . \qquad (12)$$

In addition to the three isotopes ^{235}U, ^{239}Pu, ^{241}Pu also ^{238}U gives a contribution of a few percent to the reactor anti-neutrino flux. For this isotope no measurements exist and one has to rely on theoretical calculations [20,21]. In the following we will always adopt for ^{238}U the parameterization with the second order polynomial given in Ref. [22], which we reproduce in the last row of Table 2. In particular, that parameterization has been used to calculate also the value of N_ℓ^ν for ^{238}U given in Table 1; the error of 2% is an educated guess motivated by the errors obtained for the other isotopes. Since no covariance matrix of the flux coefficients for ^{238}U is available we will always assume in the following that they are known exactly. Since the contribution of ^{238}U to the total flux is rather small, this assumption has very little impact on the conclusions drawn in this work.

4 The impact of anti-neutrino flux uncertainties in KamLAND

The KamLAND [6, 7] reactor neutrino experiment is located in the Kamioka mine in Japan and observes the electron anti-neutrinos emitted by ~ 16 nuclear power plants at distances of ~ 200 km. The results of KamLAND have provided convincing evidence for $\bar{\nu}_e$ disappearance and are in agreement with the so-called LMA-MSW solution of the solar neutrino problem (see, *e.g.*, Ref. [24]). The neutrino oscillation analysis of current KamLAND data is dominated by statistical errors[4] and it is and good approximation to gather various sources of systematical errors into an uncertainty on the overall number of events. However, in future, if more data are accumulated statistical errors will decrease and in principle one has to treat systematical errors more carefully. In this section we investigate the impact of uncertainties on the anti-neutrino flux for the determination of oscillation parameters in KamLAND. To this end we naively extrapolate the size of the data sample published in Ref. [6] to a total of five years data taking time by multiplying the event numbers by the factor $5 \times 356/145.1$, where 145.1 days is the exposure time of the reference sample. For further details on the KamLAND analysis see Refs. [24, 25].

In the case of KamLAND one has to generalize the expression for the number of events per positron energy bin from Eq. (3) to account for the fact that several reactors (labeled by the index r) at different distances L_r contribute to the signal, and that neutrino oscillations occur:

$$N_i = \mathcal{N} \sum_r \frac{P_r}{L_r^2} \sum_\ell \frac{f_{r\ell}}{E_\ell} \int dE_\nu \, \sigma(E_\nu) \, \phi_\ell(E_\nu) \, R_i(E_\nu) \, P_{ee}(L_r/E_\nu) \, . \tag{13}$$

Here $\mathcal{N}$ is a normalization constant, P_r and $f_{r\ell}$ are the power output and the element composition of the reactor r, respectively, and P_{ee} is the oscillation probability depending on the neutrino mass squared difference Δm^2 and the mixing angle θ. In our analysis we consider the following contributions to the covariance matrix $V^{\rm KL}$ of the event numbers N_i:

$$V_{ij}^{\rm KL} = N_i \delta_{ij} + N_i N_j \sigma_{\rm det}^2 + V_{ij}^{\rm flux} \, , \tag{14}$$

where the first term of the right hand side is the statistical error and the second term accounts for the over all normalization error $\sigma_{\rm det}$. The uncertainties on the anti-neutrino flux are included in $V^{\rm flux}$, which we take as

$$V_{ij}^{\rm flux} = \sum_r \frac{\partial N_i}{\partial P_r} \frac{\partial N_j}{\partial P_r} (\delta P_r)^2 + \sum_{r\ell} \frac{\partial N_i}{\partial f_{r\ell}} \frac{\partial N_j}{\partial f_{r\ell}} (\delta f_{r\ell})^2 + \sum_{k\ell} \frac{\partial N_i}{\partial c_{k\ell}} \frac{\partial N_j}{\partial c_{k\ell}} (\delta c_{k\ell})^2 \, . \tag{15}$$

Here δP_r and $\delta f_{r\ell}$ are the errors on the power output and isotope composition of each reactor, and we assume typical values of $(\delta P_r)/P_r = 0.02$ and $(\delta f_{r\ell})/f_{r\ell} = 0.01$. These errors are taken uncorrelated between the reactors. The last term in Eq. (15) takes into account the uncertainty on the coefficients of the parameterization for the anti-neutrino fluxes as discussed in Sec. 3.

In Figure 3 we show the 3σ allowed regions for the oscillation parameters after 5 years of KamLAND data for various assumptions about the systematic errors. We observe from this figure that even after 5 years the KamLAND analysis is dominated by the statistical and

[4] The robustness of the KamLAND results with respect to statistical fluctuations has been extensively discussed in Ref. [25].

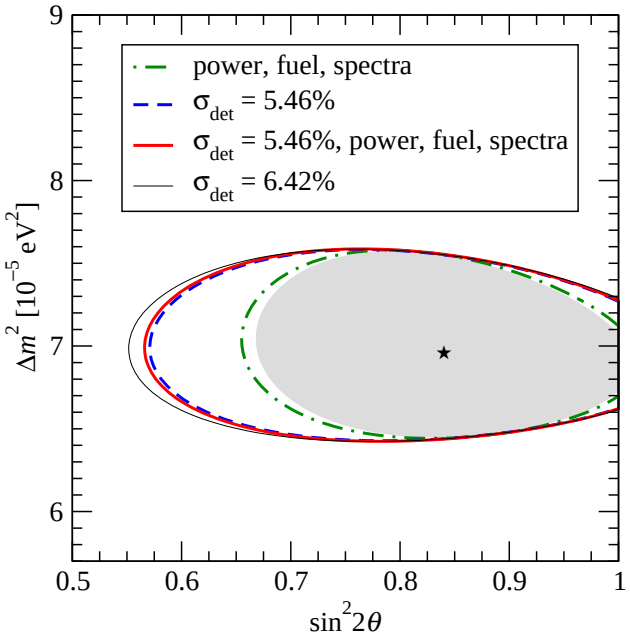

Figure 3: (Color online) 3σ allowed regions for $\sin^2 2\theta$ and Δm^2 after 5 years of KamLAND data. The shaded region corresponds to statistical errors only, the regions delimited by the curves correspond to various assumptions about systematical errors. $\sigma_{\rm det}$ is a fully correlated error on the overall normalization. For the curves labeled "power, fuel, spectra" we include a 2% error on the power output of each reactor, 1% error on the fuel composition of each reactor, and the uncertainty on the anti-neutrino spectrum as described in the text.

the overall normalization errors. The shaded region corresponds to statistical errors only, for the thin solid curve only the normalization error of $\sigma_{\rm det} = 6.42\%$ [6] is included. In Table 2 of Ref. [6] various contributions to $\sigma_{\rm det}$ are listed. If the uncertainties related to the flux are subtracted $\sigma_{\rm det}$ is reduced to 5.46% (see blue/dashed curve in Figure 3). For the red/solid and green/dash-dotted curves also the flux uncertainties according to Eq. (15) are included. In both cases we find a very small effect on the oscillation parameters.

To summarize, we find that even for 5 years of KamLAND data the determination of the oscillation parameters is dominated by statistical and overall normalization errors. The effect of flux uncertainties is rather small, and in particular it is not necessary to fully take into account flux shape errors. The inclusion of only the normalization errors for the total flux from each element (see Table 1) leads to nearly identical results as accounting for the full covariances of the coefficients $a_{k\ell}$. However, the proper treatment of the flux uncertainties reduces the overall normalization error. This will become more relevant if in future KamLAND analyses normalization errors like the uncertainty on the fiducial volume will be reduced. This will be relevant mainly for the measurement of the mixing angle, the determination of Δm^2 is hardly affected by any of the systematical errors.

Finally, we note that already for the current KamLAND data sample [7] small differences in the allowed regions are visible due to the use of our neutrino fluxes, compared to the parameterization of Ref. [22]. For completeness, we mention that additional effects like the time evolution of the individual reactor powers or isotope compositions due to burn-up [26] may become relevant for future KamLAND analyses. The investigation of such effects is

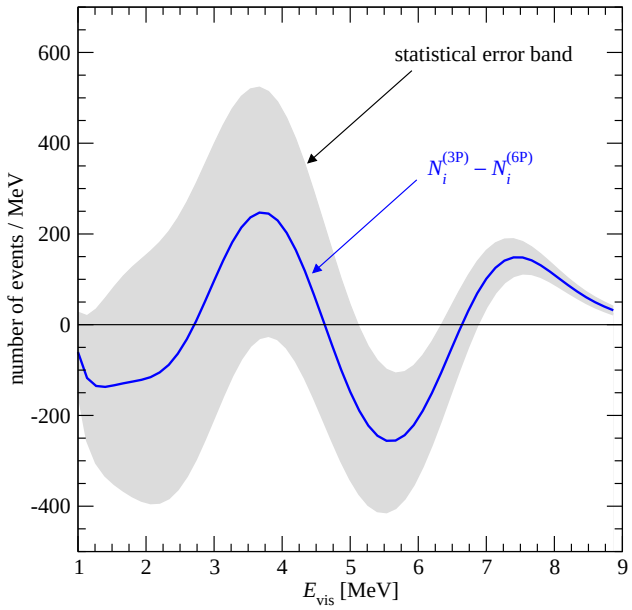

Figure 4: (Color online) Difference between the positron spectra for no oscillations $N_i^{(3P)}$ and $N_i^{(6P)}$, obtained by using the 3 parameter fit (Table 2) and 6 parameter fit (Table 3) to the anti-neutrino spectra, respectively. We assume a total number of events of 40000 and a typical isotope composition of ^{235}U : ^{239}Pu : ^{238}U : ^{241}Pu = 0.57 : 0.30 : 0.08 : 0.06. The shaded area corresponds to the 1σ statistical error band, *i.e.*, $\pm\sqrt{N_i^{(6P)}}$. For 60 bins in positron energy and statistical errors only we find $\chi^2/\text{dof} = 139/60$.

beyond the scope of the present work.

5 Application to future reactor experiments to measure θ_{13}

Let us now discuss the relevance of the flux uncertainties for reactor experiments planned to measure the small leptonic mixing angle θ_{13}. It has been realized that the bound on this angle from previous experiments [4, 5] can be significantly improved if in addition to a far detector at a distance of order 2 km from the reactor a near detector at a few hundred meters is used. Due to the large number of events, the near detector provides accurate information on the reactor neutrino flux. Identical near and far detectors with normalization errors σ_{det} below 1% will provide an accuracy on $\sin^2 2\theta_{13}$ of order 0.01 (see, *e.g.*, Refs. [9, 27–30]).

In Fig 4 we show the difference between the positron spectra predicted for no oscillations from the three and six parameter description of the neutrino spectra. The comparison with the statistical accuracy for a total number of events of 40000, which is typical for the far detector of these experiments [9], shows that for such experiments a precise model for the flux is needed. The small differences between the two parameterizations are clearly distinguishable by the statistical precision in the far detector: For 60 bins in positron energy we obtain $\chi^2/\text{dof} = 139/60$, where $\chi^2 = \sum_i [N_i^{(6P)} - N_i^{(3P)}]^2/N_i^{(6P)}$. Note that in the near detector χ^2 is much worse, because of the larger number of events.

In the following we adopt the six parameter model for the neutrino fluxes and investigate the impact of the errors of the coefficients on the sensitivity to the mixing angle. For simplicity we consider here only two-flavour neutrino oscillations characterized by the mixing

angle θ and the neutrino mass-squared difference Δm^2. The number of events in a given positron energy bin i in the detector A ($A = N, F$) can be calculated by

$$N_i^A = P \frac{\mathcal{N}_A}{L_A^2} \sum_\ell \frac{f_\ell}{E_\ell} \int dE_\nu \, \sigma(E_\nu) \, \phi_\ell(E_\nu) \, R_i(E_\nu) \, P_{ee}(L_A/E_\nu) \, . \tag{16}$$

Similar to Ref. [27] we take into account the various systematical errors by writing

$$T_i^A = (1 + a + b_A) N_i^A + g_A M_i^A + \sum_\ell \zeta_\ell \, f_\ell \, \frac{\partial N_i^A}{\partial f_\ell} + \sum_{k\ell} \xi_{k\ell} \, \delta c_{k\ell} \frac{\partial N_i^A}{\partial c_{k\ell}} \, . \tag{17}$$

Here the parameters a and b_A describe the uncertainty on the reactor power and the detector normalizations, respectively. The term $g_A M_i^A$ accounts for the energy calibration (see Ref. [27] for details) and the last two terms in Eq. (17) describe the uncertainty on the isotope fractions and the coefficients $c_{k\ell}$, respectively. To test the oscillation parameters we consider the χ^2

$$\chi^2 = \sum_{i,A} \frac{\left(T_i^A - O_i^A\right)^2}{O_i^A} + \left(\frac{a}{\sigma_a}\right)^2 + \sum_A \left[\left(\frac{b_A}{\sigma_{\rm det}}\right)^2 + \left(\frac{g_A}{\sigma_{\rm cal}}\right)^2 \right] + \sum_\ell \left(\frac{\zeta_\ell}{\sigma_f}\right)^2 + \sum_{k\ell} \xi_{k\ell}^2 \, , \tag{18}$$

where the T_i^A depend on θ and Δm^2, whereas $O_i^A = N_i^A(\theta = \Delta m^2 = 0)$. For each value of θ and Δm^2 Eq. (18) has to be minimized with respect to the "pulls" $a, b_A, g_A, \zeta_\ell, \xi_{k\ell}$.

In Figure 5 we show the results of this analysis for a wide range of Δm^2. The values of Δm^2 relevant for the θ_{13} measurement are constrained by atmospheric neutrino data to the interval $1.4{\cdot}10^{-3}\,\mathrm{eV}^2 \leq \Delta m^2 \leq 3.6{\cdot}10^{-3}\,\mathrm{eV}^2$ at 3σ (shaded region in Figure 5). The regions of Δm^2 up to $1\,\mathrm{eV}^2$ could be relevant for oscillations into hypothetical sterile neutrinos [31,32]. The solid curves in Figure 5 are calculated for perfectly known anti-neutrino flux, *i.e.*, by fixing the coefficients $\xi_{k\ell}$ in Eqs. (17) and (18) to zero. For the dashed curves we use the errors obtained in the fit to the beta spectra as discussed in Sec. 3. For the dotted curves the anti-neutrino flux coefficients are treated as free parameters in the fit, *i.e.*, we drop the last term in Eq. (18) when minimizing with respect to $\xi_{k\ell}$. In Figure 5 we consider two experimental configurations. One corresponds to an experiment with $6 \cdot 10^4$ events in the far detector for no oscillations and near and far detector baselines of $L_{\rm ND} = 0.15\,\mathrm{km}$ and $L_{\rm FD} = 1.05\,\mathrm{km}$. This set-up is similar to the Double-Chooz proposal [30]. For the second configuration we have assumed a somewhat larger near detector baseline of $L_{\rm ND} = 0.7\,\mathrm{km}$, a far detector baseline optimized for $\Delta m^2 \sim 2 \cdot 10^{-3}\,\mathrm{eV}^2$ of $L_{\rm ND} = 1.7\,\mathrm{km}$, and a rather high luminosity of $6 \cdot 10^5$ events.

Let us first discuss the region of Δm^2 relevant for the θ_{13} measurement. We observe from the figure that in the case of $L_{\rm ND} = 0.15\,\mathrm{km}$ the limit does hardly depend on the assumptions concerning the flux uncertainty. Even the flux free limit is not much worse than the limit for no error on the flux, since at these short distances the near detector provides a very accurate determination of the anti-neutrino flux. In contrast, the flux uncertainty has some impact on the θ_{13} measurement if the near detector baseline is somewhat larger. In that case oscillations start to build up already between reactor and near detector and the uncertainties on the initial flux become relevant (see also Figure 12 in Ref. [27]). In the region $\Delta m^2 \gtrsim 5{\cdot}10^{-3}\,\mathrm{eV}^2$ the main information relevant for the limit is provided by the near detector. Hence the flux uncertainties become even more relevant for both configurations in that region. We note

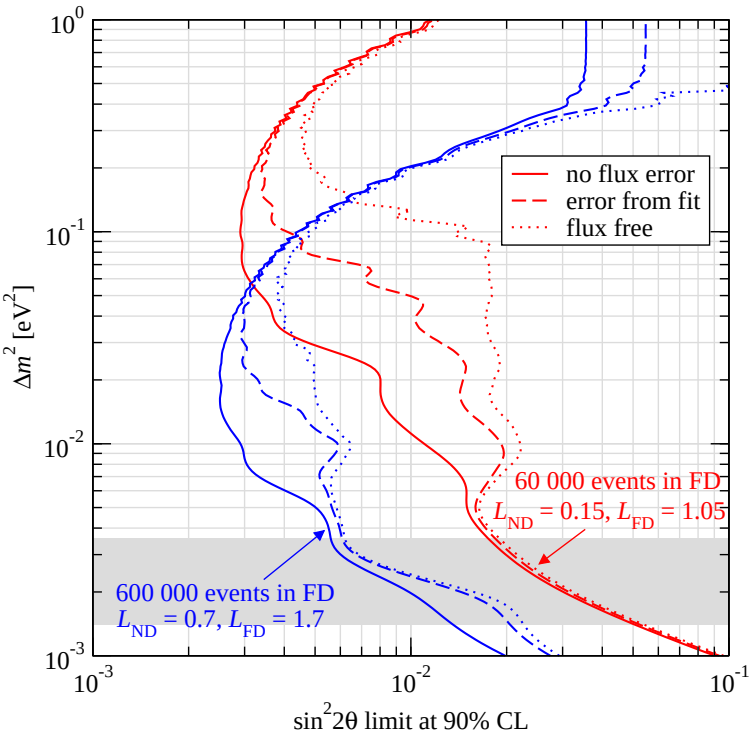

Figure 5: (Color online) The 90% CL limit on $\sin^2 2\theta$ from reactor neutrino experiments with near and far detectors as a function of Δm^2. The bound is shown for two experimental configurations as indicated in the figure. The solid curves correspond to no errors on the reactor neutrino flux, for the dashed curves the covariance matrix from the fit to the beta spectra is used, and for the dotted curves the coefficients for the anti-neutrino flux are treated as free parameters in the fit. In all cases we have assumed $\sigma_a = 1\%$ for the uncertainty of the reactor power, $\sigma_{\rm det} = 0.6\%$ for the detector normalization, $\sigma_{\rm cal} = 0.5\%$ for the energy calibration, and $\sigma_f = 1\%$ for the error on the isotope fractions. The shaded region indicates the range of Δm^2 allowed at 3σ from atmospheric neutrino data.

that around $\Delta m^2 \sim 2\,(7) \cdot 10^{-1}\,\mathrm{eV}^2$ for the big (small) experiment the limit again becomes independent of the flux uncertainty. In that region rather fast oscillations occur at the near detector which still can be resolved by the detector, but cannot be mimicked by adjusting the coefficients of the flux parameterization. Obviously, no limit can be obtained for the flux free analysis in the averaging regime of very high Δm^2.

6 Potential of an anti-neutrino detector close to a reactor

In this section we investigate the potential of an anti-neutrino detector very close to a reactor, where "very close" is defined by the requirement that neutrino oscillations do not occur. This could be for example a near detector of the experiments considered in the previous section, if it is situated close enough to the reactor. In Subsec. 6.1 we investigate to what extent the uncertainty on the anti-neutrino flux can be reduced by such a measurement, whereas in Subsec. 6.2 we consider the possibility to determine the isotope composition of the reactor core.

To this aim we write the theoretical prediction for the number of events in bin i given in

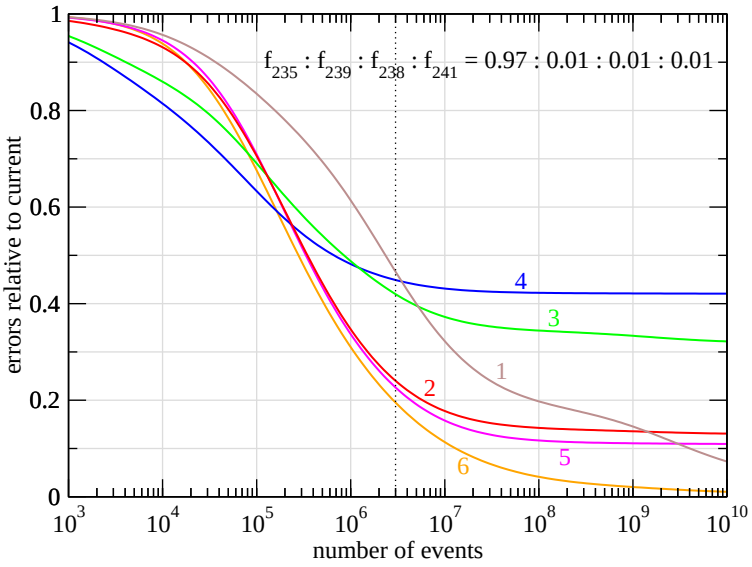

Figure 6: (Color online) Improvement for the anti-neutrino flux errors for ^{235}U as a function of the total number of events in a detector close to a reactor. We show $\sqrt{S^{\rm new}_{\alpha\alpha}}$, where $S^{\rm new}$ is defined in Eq. (21) and α runs over the 6 pulls associated with the flux-uncertainties shown in Fig. 2. We assume that the core contains 97% ^{235}U, and we take $\sigma_a = 1\%$, $\sigma_{\rm det} = 0.6\%$, $\sigma_{\rm cal} = 0.5\%$, and $\sigma_f = 1\%$. The dotted line corresponds roughly to the number of events expected in the near detector of the Double-Chooz experiment [30].

Eq. (17) as

$$T_i = O_i + \sum_\alpha p_\alpha \Phi^i_\alpha \,, \tag{19}$$

where we drop the detector index A and we use the fact that $N_i = O_i$ for no oscillations. The index α runs over all the pulls: $p_\alpha = (a, b, g, \zeta_\ell, \xi_{k\ell})$ and the coefficients Φ^i_α can be read off from Eq. (17). With this notation Eq. (18) becomes

$$\chi^2 = \sum_i \frac{\left(\sum_\alpha p_\alpha \Phi^i_\alpha\right)^2}{O_i} + \sum_\alpha \left(\frac{p_\alpha}{\delta p_\alpha}\right)^2 \,, \tag{20}$$

where δp_α is the error on the pull p_α, which can be read off from Eq. (18). Departing from Eq. (20) it is straight forward to compute the improvement of the knowledge on a given parameter p_α due to the data O_i: Because of the quadratic structure of Eq. (20) the new covariance matrix $S^{\rm new}$ of the p_α can be obtained by inverting

$$(S^{\rm new})^{-1}_{\alpha\beta} = \frac{1}{2}\frac{\partial^2\chi^2}{\partial p_\alpha \partial p_\beta} = \delta_{\alpha\beta}\frac{1}{(\delta p_\alpha)^2} + \sum_i \frac{\Phi^i_\alpha \Phi^i_\beta}{O_i} \,. \tag{21}$$

Note that in general the p_α will be correlated after the measurement, *i.e.*, $S^{\rm new}$ will aquire non-diagonal entries from the second term in Eq. (21). The final one sigma error on a parameter p_α is given by $\sqrt{S^{\rm new}_{\alpha\alpha}}$.

6.1 Improving our knowledge on the anti-neutrino flux

From Figure 5 one can see that the limit on the mixing angle is nearly the same for an analysis with completely free anti-neutrino flux coefficients (dotted curves) and for the current errors on them (dashed curves), in the region $\Delta m^2 \lesssim 10^{-2}\,{\rm eV}^2$, where oscillations can

be neglected in the near detector. This indicates that the near detector provides a rather precise determination of the flux on its own.

This fact is quantified in Figure 6, where we show the improvement of the flux errors for ^{235}U from the near detector data with respect to the present errors obtained from the fit to the beta spectra measurements. We observe from the figure that for a number of events $\gtrsim 10^4$ the errors on the flux coefficients from the anti-neutrino measurement become comparable to the current errors. To reduce the errors by a factor two roughly 10^7 events are needed. To avoid correlations with the flux coefficients from other isotopes, we assume that the core contains practically only ^{235}U. However, for large number of events the errors on the coefficients $c_{k\ell}$ become strongly correlated. Especially the coefficients corresponding to the lines labeled "2", "3" and "4" in Figure 6 are nearly fully correlated. This implies that a certain combination of these coefficients is severely constrained, and one should perform a diagonalization of the covariance matrix (similar as described in Section 3) to obtain again uncorrelated flux uncertainties in analogy to Figure 2. Note that the modes labeled "5" and "6" corresponding to relatively "fast oscillations" (compare Figure 2) can be determined rather good by the anti-neutrino measurement. We find only modest correlations of these coefficients.

In general also sizable fractions of ^{239}Pu, ^{241}Pu and ^{238}U will be present in the reactor. In this case all coefficients will become correlated. It might be possible to disentangle the contributions of the various isotopes taking into account precise information on the time evolution of the reactor composition. The improvement for a given isotope depends strongly on the relative amount of this isotope in the core.

6.2 Determination of the isotope composition of a reactor

In this subsection we investigate the possibility to determine the isotope composition of a reactor core by a nearby anti-neutrino detector. This could lead to applications of neutrino spectroscopy for reactor monitoring, either for improving the reliability of operation of power reactors or as a method to accomplish certain safeguard and non-proliferation objectives. In both cases the price tag of a moderately sized detector is small compared to the overall cost or benefit. Therefore the applicability of neutrino spectroscopy seems to depend only on its performance compared to existing technologies. For example the accuracy in the determination of the thermal power of civil power reactors as used for the production of electricity typically is in the range $0.6\% - 1.5\%$ [5]. The isotopic composition usually is not measured in situ but deduced from the time development of the reactor thermal power and the initial isotopic composition by using detailed reactor core simulation tools and is typically accurate at the percent level [11].

On the other hand, one requires for safeguard purposes to achieve a sensitivity which allows to quickly detect the diversion of weapons grade material at the level of one critical mass [10], *e.g.* for Plutonium this is approximately 10 kg. The average power reactor contains three tons of fissionable material of which roughly 40% have been converted to Plutonium by the end of the fuel life time, thus 10 kg Plutonium correspond to $\sim 0.8\%$ of the total content of Plutonium, which is beyond the accuracy levels for in situ monitoring today. The determination of the isotopic composition by the traditional methods furthermore relies on the assumption that the operator of the reactor collaborates. In the following we will show

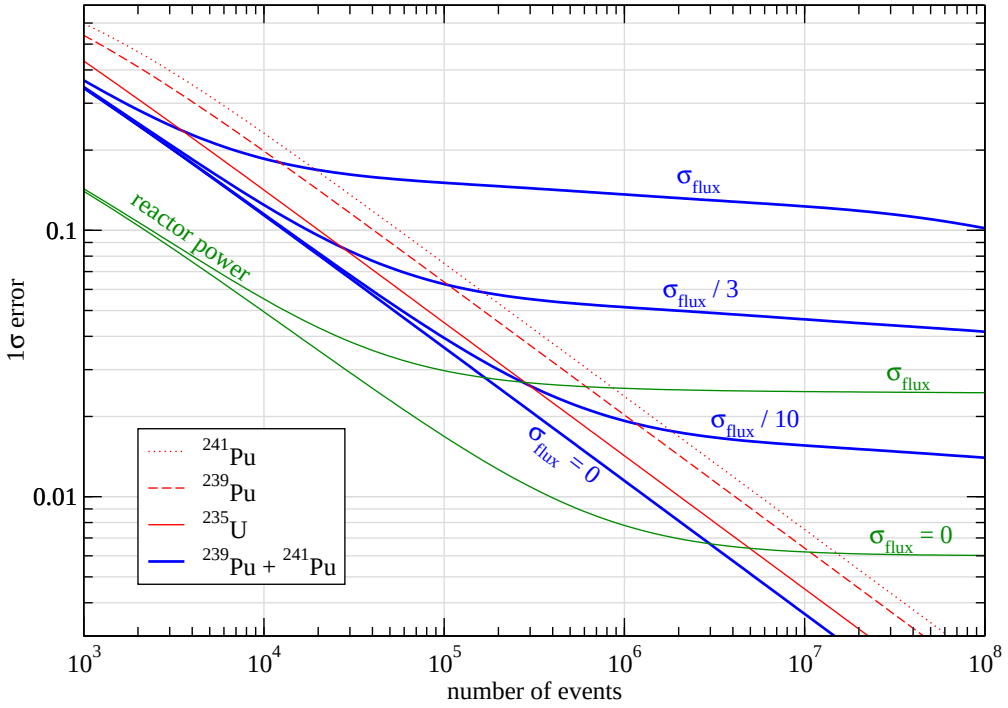

Figure 7: (Color online) The 1σ error on the fraction of ^{235}U, ^{239}Pu, and ^{241}Pu as a function of the number of anti-neutrino events. The think curves correspond to the error on the sum of ^{239}Pu and ^{241}Pu. The straight lines are calculated for perfectly known anti-neutrino fluxes. For the sum of ^{239}Pu and ^{241}Pu we show also the result assuming the present anti-neutrino flux uncertainties ("$\sigma_{\rm flux}$"), and uncertainties reduced by factors three ("$\sigma_{\rm flux}/3$") and ten ("$\sigma_{\rm flux}/10$"). Also shown is the relative 1σ error on the reactor power for $\sigma_{\rm flux} = 0$ and present flux errors. We assume an isotope composition $^{235}\mathrm{U} : {}^{239}\mathrm{Pu} : {}^{238}\mathrm{U} : {}^{241}\mathrm{Pu} = 0.4 : 0.4 : 0.1 : 0.1$ and a detector normalization uncertainty $\sigma_{\rm det} = 0.6\%$.

that neutrino spectroscopy has the potential to reach a sensitivity comparable to existing technologies and it does *not* require detailed information on the power history or the initial fuel composition, which is an important advantage especially in safeguards applications. In contrast to the existing literature on this topic [10–12] we use the full spectral information and therefore do not require an independent determination of the reactor power. In general, any safeguard regime based only on the total rate suffers from two problems: The first one is related to the availability of reliable information on the thermal power, whereas the second one is related to the fact that for most reactor types the diversion of core inventory is only possible during refueling, *i.e.* when the reactor is switched off and there is no neutrino flux. Thus in order to detect any diversion in this period an absolute measurement of the neutrino flux as well as of the thermal power is required. Moreover the composition of the new fuel has to be known exactly in order to predict the spectrum which is expected in case of no diversion.

In the following we perform a fit where the isotope fractions f_ℓ are treated as free parameters, subject to the condition $\sum f_\ell = 1$. We impose no external information on the reactor power, *i.e.*, no knowledge at all about the reactor is assumed. This means that we set $1/(\delta p_\alpha)^2 = 0$ in Eq. (21) for α corresponding to σ_a and σ_f. The determination of the isotope fractions and the power is solely based on the differences between the anti-neutrino spectra emitted by the four isotopes. In Figure 7 we show the 1σ accuracy obtained on the

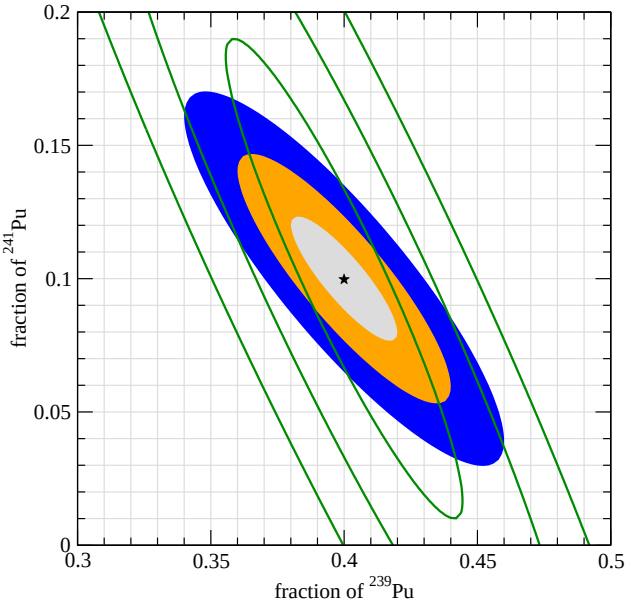

Figure 8: (Color online) Contours of $\Delta\chi^2 = 1, 4, 9$ in the plane of the ^{239}Pu and ^{241}Pu isotope fractions for 10^6 anti-neutrino events. The colored regions correspond to perfectly known anti-neutrino flux shapes, whereas for the curves we assume uncertainties on the flux coefficients three times smaller than the present errors. We adopt the same isotope composition and $\sigma_{\rm det}$ as in Figure 7. Reactor power and ^{235}U fraction are treated as a free parameters.

isotope fractions and the reactor power as a function of the anti-neutrino events. To give an example, for a detector with one ton fiducial mass at a distance of ten meters from a reactor with three GW thermal power roughly 10^6 events are expected within 3 months of measurement time.

First, one can see from Figure 7 that for $\gtrsim 10^5$ events a rather precise determination of the reactor power at the $\lesssim 3\%$ level is possible, given the current uncertainty on the anti-neutrino fluxes. For perfectly known fluxes the power accuracy is limited by the systematical uncertainty of the detector normalization. Second, for $\gtrsim 10^6$ events also the isotope fractions of ^{235}U, ^{239}Pu, and ^{241}Pu can be determined at the percent level if no errors on the anti-neutrino fluxes are taken into account.[5] The accuracy on the sum of the ^{239}Pu and ^{241}Pu fractions is clearly better than the one on the individual fractions. This is a consequence of the strong anti-correlation between the two Pu isotopes, which we illustrate in Figure 8, where χ^2 contours in the ^{239}Pu–^{241}Pu plane are shown for 10^6 events. Note that for safeguard applications actually the sum of both Plutonium isotopes is the interesting quantity.

From Figure 7 one can see that to determine the isotope composition a precise knowledge of the emitted fluxes is necessary. With present errors the 1σ accuracy is limited to $\gtrsim 10\%$. To reach a determination at the percent level the errors on the coefficients of the flux parameterization have to be reduced by a factor of three to ten. A factor three would be approximately achieved by the near detector of an experiment like Double-Chooz [30].

Let us note that in this analysis we do not take into account additional information such as the time evolution and reactor burn-up, or information from various traditional safeguard

[5] We consider the fractions of ^{235}U, ^{239}Pu, and ^{241}Pu as independent parameters, and determine the ^{238}U fraction by the constraint $\sum f_\ell = 1$.

methods. The main conclusion from the above results is that anti-neutrino spectroscopy may play an important role for reactor monitoring, especially since one expects significant synergies due to the combination with alternative technologies.

7 Summary and conclusions

In this work we have presented an accurate parameterization of the anti-neutrino flux produced by the isotopes ^{235}U, ^{239}Pu, and ^{241}Pu in nuclear reactors. We use a polynomial of order 5 and determine the coefficients by performing a fit to spectra inferred from experimentally measured beta spectra. Furthermore, the correlated errors on these coefficients are determined from the fit.

Subsequently we investigate the impact of the flux uncertainties for the KamLAND experiment and future reactor experiments to measure the mixing angle θ_{13}. We show that flux shape uncertainties can be safely neglected in the KamLAND experiment, however the proper treatment of the errors associated to the anti-neutrino flux reduces somewhat the overall systematic error in KamLAND, which has some impact on the determination of the mixing angle. Future high precision reactor neutrino experiments with a far detector at distances of order 2 km and a near detector at hundreds of meters are sensitive to the fine details of the reactor neutrino spectra. We find that a parameterization based on a polynomial of order two is not accurate enough to describe the anti-neutrino spectrum at the required level of precision. If the near detector is located at distances $\gtrsim 500$ meters the flux uncertainties are relevant for the θ_{13} measurements. Moreover, in searches for sterile neutrinos at values of $\Delta m^2 \gtrsim 10^{-2}\,\mathrm{eV}^2$ the main information is provided by the near detector, and hence the inclusion of anti-neutrino flux uncertainties is essential.

Finally, we have investigated the potential of a detector very close to a reactor to improve on the uncertainties of the anti-neutrino fluxes, and to determine the isotopic composition in nuclear reactors through an anti-neutrino measurement. We find that without any external knowledge on the reactor a three month exposure of a one ton detector allows the determination of the isotope fractions and the thermal reactor power at a few percent accuracy. This may open the possibility of an application for safeguard or non-proliferation objectives, which does not rely on information on the reactor thermal power or on the initial fuel composition, and hence neutrino spectroscopy can provide information complementary to traditional monitoring methods. To achieve this goal a reduction of the present errors on the anti-neutrino fluxes of about a factor of three is necessary, which naturally can be obtained from the data of the near detector of a Double-Chooz like experiment.

Acknowledgments

We thank Michele Maltoni for discussions on the KamLAND analysis, and Hervé de Kerret for communication on the CHOOZ experiment. This work has been supported by the "Sonderforschungsbereich 375 für Astro-Teilchenphysik der Deutschen Forschungsgemeinschaft".

A Results of the fits to the anti-neutrino spectra

In this appendix we give the best-fit coefficients for the polynomials used to parameterize the anti-neutrino flux of the isotopes ^{235}U, ^{239}Pu, and ^{241}Pu according to Eq. (4). In Table 2 the coefficients for the polynomial of order 2 are given, wheres in Table 3 we display the coefficients, their errors and the correlation matrix for the polynomial of order 5.

ℓ	$a_{1\ell}$	$a_{2\ell}$	$a_{3\ell}$
^{235}U	0.904	−0.184	−0.0878
^{239}Pu	1.162	−0.392	−0.0790
^{241}Pu	0.852	−0.126	−0.1037
^{238}U	0.976	−0.162	−0.0790

Table 2: Coefficients of the polynomial of order 2. For ^{235}U, ^{239}Pu, ^{241}Pu the numbers are obtained from a fit to the data from Refs. [16, 17], for ^{238}U we reproduce the values given in Ref. [22].

$\ell = {}^{235}$U			correlation matrix $\rho^{\ell}_{kk'}$					
k	$a_{k\ell}$	$\delta a_{k\ell}$	1	2	3	4	5	6
1	$3.519 \cdot 10^{0}$	$7.26 \cdot 10^{-1}$	1.000	−0.996	0.987	−0.973	0.956	−0.938
2	$-3.517 \cdot 10^{0}$	$8.81 \cdot 10^{-1}$	−0.996	1.000	−0.997	0.989	−0.976	0.962
3	$1.595 \cdot 10^{0}$	$4.06 \cdot 10^{-1}$	0.987	−0.997	1.000	−0.997	0.990	−0.980
4	$-4.171 \cdot 10^{-1}$	$8.90 \cdot 10^{-2}$	−0.973	0.989	−0.997	1.000	−0.998	0.992
5	$5.004 \cdot 10^{-2}$	$9.34 \cdot 10^{-3}$	0.956	−0.976	0.990	−0.998	1.000	−0.998
6	$-2.303 \cdot 10^{-3}$	$3.77 \cdot 10^{-4}$	−0.938	0.962	−0.980	0.992	−0.998	1.000
$\ell = {}^{239}$Pu			correlation matrix $\rho^{\ell}_{kk'}$					
k	$a_{k\ell}$	$\delta a_{k\ell}$	1	2	3	4	5	6
1	$2.560 \cdot 10^{0}$	$4.01 \cdot 10^{-1}$	1.000	−0.993	0.977	−0.954	0.928	−0.899
2	$-2.654 \cdot 10^{0}$	$5.58 \cdot 10^{-1}$	−0.993	1.000	−0.995	0.982	−0.962	0.938
3	$1.256 \cdot 10^{0}$	$2.91 \cdot 10^{-1}$	0.977	−0.995	1.000	−0.996	0.984	−0.967
4	$-3.617 \cdot 10^{-1}$	$7.17 \cdot 10^{-2}$	−0.954	0.982	−0.996	1.000	−0.996	0.986
5	$4.547 \cdot 10^{-2}$	$8.37 \cdot 10^{-3}$	0.928	−0.962	0.984	−0.996	1.000	−0.997
6	$-2.143 \cdot 10^{-3}$	$3.73 \cdot 10^{-4}$	−0.899	0.938	−0.967	0.986	−0.997	1.000
$\ell = {}^{241}$Pu			correlation matrix $\rho^{\ell}_{kk'}$					
k	$a_{k\ell}$	$\delta a_{k\ell}$	1	2	3	4	5	6
1	$1.487 \cdot 10^{0}$	$3.23 \cdot 10^{-1}$	1.000	−0.991	0.974	−0.950	0.923	−0.893
2	$-1.038 \cdot 10^{0}$	$4.31 \cdot 10^{-1}$	−0.991	1.000	−0.994	0.980	−0.960	0.936
3	$4.130 \cdot 10^{-1}$	$2.15 \cdot 10^{-1}$	0.974	−0.994	1.000	−0.995	0.984	−0.966
4	$-1.423 \cdot 10^{-1}$	$5.02 \cdot 10^{-2}$	−0.950	0.980	−0.995	1.000	−0.996	0.986
5	$1.866 \cdot 10^{-2}$	$5.54 \cdot 10^{-3}$	0.923	−0.960	0.984	−0.996	1.000	−0.997
6	$-9.229 \cdot 10^{-4}$	$2.33 \cdot 10^{-4}$	−0.893	0.936	−0.966	0.986	−0.997	1.000

Table 3: Coefficients $a_{k\ell}$ of the polynomial of order 5 for the anti-neutrino flux from elements $\ell = {}^{235}$U, ^{239}Pu, and ^{241}Pu. In the column $\delta a_{k\ell}$ the 1σ errors on $a_{k\ell}$ are given. Furthermore the correlation matrix of the errors is shown.

References

[1] C. L. Cowan, F. Reines, F. B. Harrison, H. W. Kruse, and A. D. McGuire, Science **124**, 103 (1956).

[2] G. Zacek *et al.* (CALTECH-SIN-TUM), Phys. Rev. **D34**, 2621 (1986).

[3] Y. Declais *et al.*, Nucl. Phys. **B434**, 503 (1995).

[4] F. Boehm *et al.*, Phys. Rev. **D64**, 112001 (2001), `hep-ex/0107009`.

[5] M. Apollonio *et al.*, Eur. Phys. J. **C27**, 331 (2003), `hep-ex/0301017`.

[6] K. Eguchi *et al.* (KamLAND), Phys. Rev. Lett. **90**, 021802 (2003), `hep-ex/0212021`.

[7] T. Araki *et al.* (KamLAND) (2004), `hep-ex/0406035`.

[8] C. Bemporad, G. Gratta, and P. Vogel, Rev. Mod. Phys. **74**, 297 (2002), `hep-ph/0107277`.

[9] K. Anderson *et al.* (2004), hep-ex/0402041.

[10] A. Bernstein, Y. Wang, G. Gratta, and T. West, J. Appl. Phys. **91**, 4672 (2002), nucl-ex/0108001.

[11] M. M. Nieto, A. C. Hayes, C. M. Teeter, W. B. Wilson, and W. D. Stanbro (2003), nucl-th/0309018.

[12] V. D. Rusov, T. N. Zelentsova, V. A. Tarasov, and D. A. Litvinov (2004), hep-ph/0403207.

[13] P. Vogel and J. F. Beacom, Phys. Rev. **D60**, 053003 (1999), hep-ph/9903554.

[14] V. I. Kopeikin, L. A. Mikaelyan, and V. V. Sinev, Phys. Atom. Nucl. **60**, 172 (1997).

[15] V. Kopeikin, L. Mikaelyan, and V. Sinev (2003), hep-ph/0308186.

[16] K. Schreckenbach, G. Colvin, W. Gelletly, and F. Von Feilitzsch, Phys. Lett. **B160**, 325 (1985).

[17] A. A. Hahn *et al.*, Phys. Lett. **B218**, 365 (1989).

[18] F. Von Feilitzsch, A. A. Hahn, and K. Schreckenbach, Phys. Lett. **B118**, 162 (1982).

[19] B. Achkar *et al.*, Phys. Lett. **B374**, 243 (1996).

[20] P. Vogel, G. K. Schenter, F. M. Mann, and R. E. Schenter, Phys. Rev. **C24**, 1543 (1981).

[21] H. V. Klapdor and J. Metzinger, Phys. Lett. **B112**, 22 (1982).

[22] P. Vogel and J. Engel, Phys. Rev. **D39**, 3378 (1989).

[23] Webpage: http://www.ph.tum.de/∼schwetz/reactor-neutrino-data/ .

[24] M. Maltoni, T. Schwetz, and J. W. F. Valle, Phys. Rev. **D67**, 093003 (2003), hep-ph/0212129.

[25] T. Schwetz, Phys. Lett. **B577**, 120 (2003), hep-ph/0308003.

[26] H. Murayama and A. Pierce, Phys. Rev. **D65**, 013012 (2002), hep-ph/0012075.

[27] P. Huber, M. Lindner, T. Schwetz, and W. Winter, Nucl. Phys. **B665**, 487 (2003), hep-ph/0303232.

[28] H. Minakata, H. Sugiyama, O. Yasuda, K. Inoue, and F. Suekane, Phys. Rev. **D68**, 033017 (2003), hep-ph/0211111.

[29] V. Martemyanov, L. Mikaelyan, V. Sinev, V. Kopeikin, and Y. Kozlov, Phys. Atom. Nucl. **66**, 1934 (2003), hep-ex/0211070.

[30] F. Ardellier *et al.* (2004), hep-ex/0405032.

[31] L. Mikaelyan and V. Sinev, Phys. Atom. Nucl. **62**, 2008 (1999), hep-ph/9811228.

[32] V. Kopeikin, L. Mikaelyan, and V. Sinev (2003), hep-ph/0310246.